Asian Journal of Physics
Vol. 30, No 6 (2021) 917-931
Available on: www.asianjournalofphysics.com

ap

Undoped and iron doped $Bi_{12}SiO_{20}$ crystals as optical limiters

P Prem Kiran

School of Physics, University of Hyderabad,

Prof. C.R. Rao Road, Gachibowli, Hyderabad – 500 046, Telangana State, India.

Dedicated to Professor D N Rao for his significant contributions and pioneering works in the fields of spectroscopy, optics, nonlinear optics and photonics

This paper reviews the potential of photorefractive single crystals for optical limiting applications and highlights the optical limiting characteristics of undoped and iron doped $Bi_{12}SiO_{20}$ (BSO), a photorefractive single crystal belonging to Sillenite family. The contribution of two-photon absorption from two channels: first from valence band to conduction band and the other from an extrinsic silicon-vacancy to conduction band assisted by charge carrier absorption from the trap states of BSO is presented. These processes lead to highly effective nonlinear absorption across the visible region of the electromagnetic spectrum. The specific role of iron doping in enhancing the effective nonlinear absorption by charge carriers as well as intraband absorption for ns laser pulses at three different excitation wavelengths of 532, 600 and 683 nm is discussed.

Keywords: $Bi_{12}SiO_{20}$ single crystal, Optical limiter, Nonlinear absorption, effective two-photon absorption, Trap level assisted Charge carrier absorption.

1 Introduction

Optical limiter, an optical analogue of electrical limiter used to safeguard many electrical devices, works in the optical region of the electromagnetic spectrum by exploiting the nonlinearities of the materials. With the advent of high-power laser sources over wide range of wavelengths and pulse durations, the necessity for protection of sensors and eyes has enormously increased over the last few decades [1,2]. In this context, optical limiters have received significant attention over the past few decades [3-16]. An ideal limiter exhibits a linear transmission below a threshold and clamps the output to a constant above it, thus providing safety to sensors or eyes. The minimum criteria identified for a material to act as an effective optical limiter are (i) Low limiting threshold and large dynamic range (ii) High optical damage threshold and stability (iii) Sensitive broadband response to long and short pulses (iv) Fast response time (v) High linear transmittance throughout the sensor band width, optical clarity, and robustness [17,18]. Wide variety of organic and inorganic materials are being studied to achieve efficient optical limiting [19]. Various approaches have been developed towards better optical limiting based on, e.g., electro-optical [20], magneto-optical [21], and all-optical [22-26] mechanisms. The all-optical limiters rely on materials that exhibit one or more of the nonlinear optical mechanisms like: Two-photon absorption (TPA), Reverse Saturable Absorption (RSA), Free carrier absorption, Thermal defocusing and scattering, Photorefraction, Nonlinear refraction, Induced scattering [27]. Enhancement in optical limiting has also been achieved by coupling two or more of these mechanisms, like Self-defocusing in conjunction with TPA [28], TPA of one molecule with excited state absorption (ESA) in another molecule [29]. Different experimental geometries like cascaded limiters [30,31], nanofluids [32] have been also studied to achieve large figure of merit and dynamic range [3-16].

Corresponding author
e mail: prem@uohyd.ac.in (P Prem Kiran)
doi: https://doi.org/10.54955/AJP.30.6.2021.917-931

The first experimental demonstration of optical power limiter reported by Leite *et al* [33] is based on the laser induced thermal lens effect using 488 nm cw Ar^+ laser beam as incident light and nitrobenzene as the linearly absorbing medium with an aperture in front of the detector. Though the change of power through the aperture was only 3% of the total input power change at high input levels, the original idea and setup is still the basis of most popular optical limiting designs using organic dye solutions [34-42], semiconductors [43-46] and other materials [47,54] as linearly absorbing media. Despite the wide varieties of semiconductor [41-57] and organic systems like modified porphyrins, pthalocyanines [58-61], arrays of Porphyrins [62,63], metal nanoclusters [64,65], binary/ternary semiconductor nanocrystals, core-shell nanocrystals [66-69], nano particles of the oxide nanocrystals [70,71] studied for optical limiting properties, bulk photorefractive materials have a significant place owing to their significant band structure in addition to the electro-optic and photoconductive capability. In the present review, the optical limiting characteristics of photorefractive crystals are discussed and a quantitative model based on the band theory explaining the unexplored nonlinear absorption characteristics of BSO crystals is presented.

2 Photorefractive materials for nonlinear optical applications

Photorefractive materials are a class of electro-optic photoconductive materials with many interesting phenomena, and applications in nonlinear optics and photonics which include phase conjugation, optical interconnections, optical spatial solitons, and optical signal processing [72-77]. The phenomenon of photorefraction arises on the nonuniform illumination of such materials and with the diffusion of the ensuing photogenerated carriers towards lesser-illuminated regions with the associated electric fields that, through the Pockels effect, cause localized changes in the refractive index. This photoionization occurs from relatively deep energy levels within the bandgap that are not normally thermally ionized. The light induced absorption due to the photoinduced charge transport has been studied widely in the field of photorefractive nonlinear optics because it plays an important role in the construction of passive optical limiters and optical threshold elements in optical processing systems [72-77].

In photorefractive materials, at higher input intensities, the mechanism of charge carrier generation and transport process involves impurity levels which lead to the greater possibility of the combined effect of trap assisted charge carrier absorption (TACCA) and TPA [78-82]. Here, the former is an accumulative nonlinearity, which requires time for energy transfer from field to medium and hence depends on energy density deposited in the medium. This nonlinearity can also be nonlocal due to the drift or diffusion of photogenerated charge carriers in the medium and hence can in principle only depend on the input fluence. The latter is an instantaneous nonlinearity, which depends on the input light intensity, can be effective over broadband of the spectrum and for very short pulses. TPA can also act as a significant loss mechanism when a material is subjected to a strong beam of photons of energy hω, with $h\omega < Eg < 2h\omega$, where Eg is the energy gap of the material. High sensitivity optical storage by the photorefractive process using multi-photon absorption was demonstrated in $LiNbO_3$ and in KTN by Linde *et al* [84]. Permanent and reversible changes of refractive index of pure and doped $LiNbO_3$ have been obtained by multi-photon absorption that results in increased sensitivity for optical storage and holography [85].

Of all the sillenite family crystals having the general formula of $Bi_{12}MO_{20}$ where M = Si, Ge, Ti etc., $Bi_{12}SiO_{20}$ are considered attractive candidates for variety of applications due to their strong photorefractive properties. Higher photosensitivity, fast response time, comparable electro-optic coefficient with other crystals of the family and interesting piezoelectric, optically-active and many other interesting properties like beam deflection, switching, holography, phase conjugation and optical memories made BSO crystals the most sought after crystals for optical applications [72-74,86]. It has been reported that out of three non-zero electro-optic coefficients r_{41}, r_{52}, and r_{63}, the element r_{41} is important for device applications [6]. $Bi_{12}SiO_{20}$ (BSO) has cubic symmetry, belonging to point group 23. In BSO the standard photorefractive effect is based on the

absorption of photons by impurity levels. One can improve the performance by means of increasing the impurity levels by doping. In BSO, many trap levels in the energy gap predicted from the spectral response of the photoconductivity [73,74] and the traps with high concentration were observed experimentally [75]. In addition of distinguishable shallow trap levels reported, there also appears to be many overlapping levels at deep energy levels below the conduction band [74,88-90]. Attard [91] predicted the Fermi level shift in BSO via photon induced trap occupation. The shift of Fermi level is dependent on the density of trap sites in the bandgap, the radiation induced occupation density, and the energy levels of the traps. Investigations report that photorefractive materials doped with iron leads to favourable photorefractive properties such as small response time and high sensitivity [78]. It is also shown that optical properties and light induced absorption changes are affected due to iron doping [79]. Investigations on the possibilities for practical applications of sillenites have revealed that doping can conveniently be used to modify the absorption in a way suitable for the application. In BSO too, doping with various elements leads to significant changes in the electrical, photoelectrical, and optical properties. Nagao and Mimura [80] have investigated the influence of many transition metals on the transmission and photoresponse of BSO. The general conclusion made about photoresponse is that the transition metal impurities in BSO crystals quench the photoconductivity. An intuitive explanation proposed for the quenching is the formation of recombination centers [81]. When the light intensities are strong enough, effects that are caused by TPA can become important [82] and can also be enhanced by the existence of intermediate energy levels inside the forbidden bandgap because of the impurities. It is found that addition of significant amount of Fe^{3+} ions as impurities can easily change the valence state and may play a critical role in charge carrier mobility as well as intensity dependent absorption. A study to this effect [87] in pure BSO crystal examined the CW recording under applied electric field at low intensities of a CW laser.

In this special issue paper, the optical limiting behavior exhibited due to combined effect of TPA, free carrier absorption and trap assisted charge carrier absorption (TACCA) in photorefractive crystals of undoped and iron doped BSO in the visible spectral range using 6 nanosecond pulses at 532, 600 and 683 nm is presented. An excellent passive limiting behavior is demonstrated using these crystals in visible region. A quantitative modeling based on the band theory of solids accounting for the absorptive changes due to combined effect of TACCA and TPA with the precise role of the internal defects due to impurity centers present in the crystal lattice, is presented.

3 Optical limiting and nonlinear absorption characteristics of undoped and iron doped BSO crystals

In this section, we describe optical limiting and nonlinear absorption study of undoped and doped BSO crystals carried out by us. An undoped BSO crystal bought from M/s Fujian Castech Crystals Inc., China with dimensions of 10 mm×10 mm× 5 mm, and a Fe-doped BSO crystal obtained from Alabama University, USA [83] with dimensions 5 mm× 4 mm× 4 mm were used in this study [83]. These crystals were cut to have thickness of 1 mm along c-axis and used for optical limiting and nonlinear absorption studies. The surfaces of both the crystals were polished to minimize the scattering. Optical limiting studies are also done with 4 mm thick crystals. The amount of iron incorporation in the Fe-doped crystal was determined using Inductive Coupled Plasma - Atomic Emission Spectroscopy (ICP-AES). The result showed that 150-ppm Fe was incorporated in the crystal as impurity. In principle, during the growth of iron doped BSO crystals, Fe can replace either Bi or Si. However, from ICP - AES study, it was found that the doped crystal grown from melt was having no Si deficit. Hence, it can be assumed that Fe atoms occupied only the Bi sites in Fe-doped BSO crystal. The crystal structures of both pure and iron doped BSO studied using single crystal X-ray diffraction technique revealed body centered cubic structures with lattice constants of (10.0935 ± 0.003)Å and (10.0335 ± 0.006)Å, respectively. A slight variation in the lattice constant of the iron doped BSO without any change in the crystal structure from that of pure BSO crystal, confirms the doping of iron. The optical absorption spectra of undoped BSO and Fe-doped BSO, represented as BSO and BSO:Fe, respectively, are shown in Fig 1.

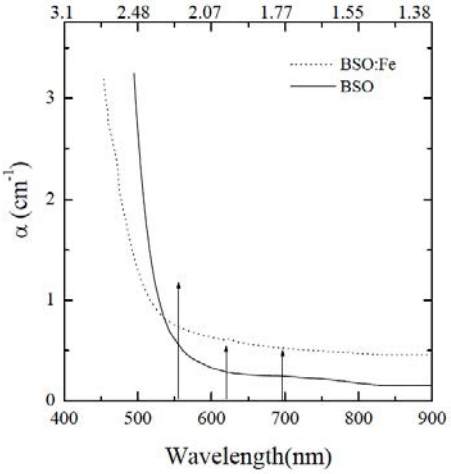

Fig 1. Absorption spectra of BSO and BSO:Fe. The three arrows represent the excitation wavelengths used in the study. Top X-axis shows the photon energy in eV.

The absorption spectra of both the crystals show a very large absorption above 3eV which matches well with the reported values [90,98]. As one can see from Fig 1 a long tail in the absorption edge goes all the way to 900 nm (1.38eV). This implies that both the crystals possess large number of donor sites. The absorption centers/traps responsible for the absorption in the above region are reported as due to either silicon vacancy complex or bismuth substituting for silicon or Fe^{3+} impurities. And these absorption centers are raised to conduction band by optical excitation with photons in energy region 1.7eV to 3.5eV [25]. The change in the absorption spectrum with various metals as dopants and different growth conditions has been reported earlier in various photorefractives like $BaTiO_3$, $LiNbO_3$ and in $PbBaNb_2O_6$ [85-87] with major variation in the visible region. Doping of impurities like iron [76], cobalt and transition metals [88] has been reported to change the optical absorption spectrum in the visible region. From the absorption coefficient the ground state absorption cross-section (σ_0) of undoped and iron doped BSO is calculated and is presented in Table 1.

Table 1. Ground state absorption cross-section of BSO and BSO:Fe at the three excitation wavelengths of 532 nm, 600 nm and 683 nm.

λ_{ex} (*nm*)	σ_0 ($\times 10^{-20}$ cm^2)	
	BSO	BSO:Fe
532	9.15	8.53
600	3.30	6.34
683	2.49	5.34

Frequency doubled Nd:YAG laser at 532 nm (Continuum 660 B-10, 10 Hz, 6 ns FWHM, 100 mJ/pulse and Spectra-Physics INDI-40, 10 Hz, 6ns 500 mJ/pulse) is used for the experimental studies of optical limiting (OL) and open aperture Z-scan studies, Figs 3-5. The second harmonic of Nd:YAG sources are used in turn to pump a RhB dye laser and a Raman Shifter filled with H_2 gas generating 600 nm and 683 nm excitation wavelength, respectively [72,89,90]. Optical limiting properties are studied by keeping the sample at the focus of f/5 geometry as a standard because human eye is equivalent to *f*/5 optical geometry [106,107]. The input energy is varied using calibrated neutral density filters, while the output is collected using a calibrated fast photodiode (FND 100). The input energy where the transmitted output becomes half of the linear transmittance is called the limiting threshold ($I_{1/2}$) of the material and an important factor for choosing a material as optical limiter. Each experimental point shown in the OL curves is an average of 128

laser pulses to get a better signal to noise ratio. The experiments are repeated to ascertain the reproducibility and to determine the error. Nonlinear absorption studies were performed using standard open-aperture Z-scan studies [93]. Optical limiting (OL) and nonlinear absorption measurements are performed with <110> direction of the crystal coinciding with the Z-axis of the beam propagation. Open aperture Z-scan studies are done with 1 mm thick crystals and OL curves are recorded with both 1 and 4 mm thick crystals. The sample satisfied the "thin" sample condition $L < n_0 z_0$, where L is the sample thickness, n_0 the linear refractive index and z_0 the diffraction length of the focused beam for Z-scan studies. No external electric field is applied across the crystal. Beam fanning is observed in the far field from BSO:Fe while performing OL and Z-scan measurements. Proper precautions are taken to collect all the transmitted light by bringing the collecting lens closer to sample and by using large diameter lens for collecting the output. Optical limiting behavior of BSO and BSO:Fe at 532 nm and 600 nm with 4 mm crystal is shown in Fig 2. The damage threshold is identified as the intensity at which a strong scattering appeared at the output followed by the darkening and a physical damage formed on the surface of the crystal. The optical limiting performance and the damage threshold have increased considerably with the presence of iron impurity. The limiting and damage thresholds of the crystals are given in Table 2.

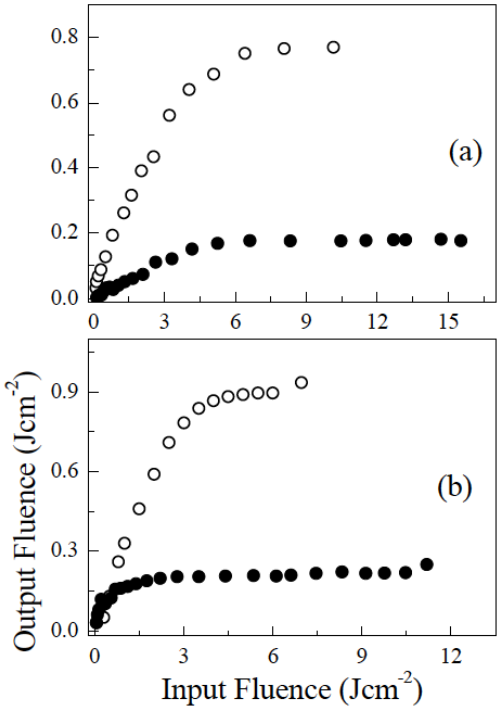

Fig 2. Optical limiting response of BSO (o) and BSO: Fe (•) at (a) 532 nm and (b) 600 nm with 4mm thick crystals.

Table 2. Ground state absorption cross-section of BSO and BSO:Fe at the three excitation wavelengths of 532 nm, 600 nm and 683 nm.

λ_{ex} (nm)	Limiting Threshold (Jcm^{-2})		Damage Threshold (Jcm^{-2})	
	BSO	BSO:Fe	BSO	BSO:Fe
532	3.38±0.4	1.29±0.2	9.6±0.3	15.6±0.2
600	5.88±0.5	3.29±0.3	6.4±0.2	10.6±0.3
683	---	---	4.7±0.2	7.7±0.3

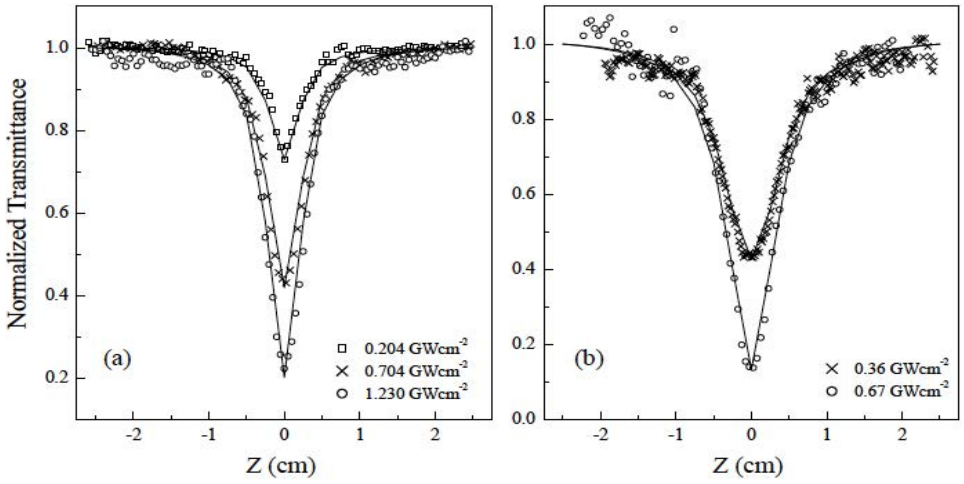

Fig 3. Open aperture Z-scan curve of (a) BSO and (b) BSO: Fe at 532 nm, 6ns pulses. Solid lines show the theoretical fits.

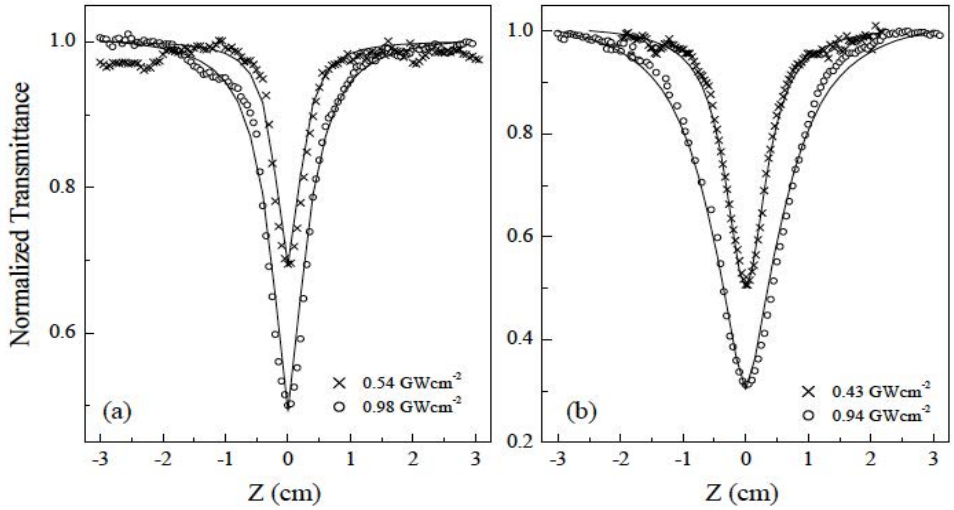

Fig 4. Open aperture Z-scan curve of (a) BSO and (b) BSO: Fe at 600 nm, 6ns pulses. Solid lines show the theoretical fits.

The limiting threshold ($I_{1/2}$) is decreasing, and the damage threshold increases with iron incorporation in these crystals. As one moves towards the longer wavelengths, the $I_{1/2}$ increases gradually and the damage threshold decreases. To understand the role of different nonlinear absorption processes leading to the observed optical limiting behaviour, the open-aperture Z-scan was performed. The nonlinear absorption behaviour of BSO and BSO:Fe at 532 nm, 600 nm and 683 nm excitation wavelengths is shown in Figs 3, 4, and 5, respectively. The symbols at the intensities as shown by the labels inside the figures represent the experimental data at the intensities as shown by the labels inside the figures. The lines overlapping the experimental data are the theoretical fits generated using equivalent five-level energy diagram of the energy band structure of BSO.

At room temperature, BSO with an optical bandgap of 3.25 eV, behaves as a two-photon absorber at 532, 600 and 683 nm as the band gap obeys $h\omega < Eg < 2h\omega$. However, the contribution of the photoinduced

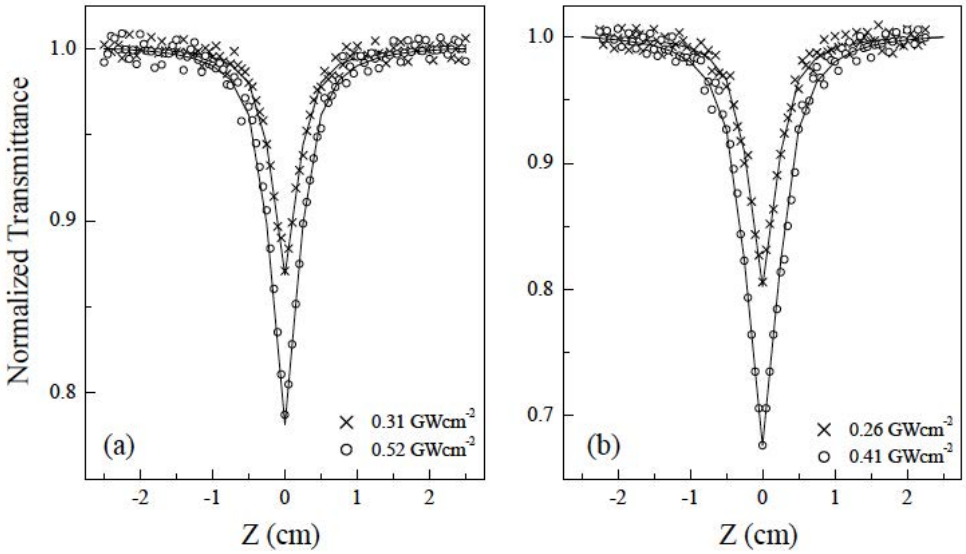

Fig 5. Open aperture Z-scan curve of (a) BSO and (b) BSO: Fe at 683 nm, 6ns pulses. Solid lines show the theoretical fits.

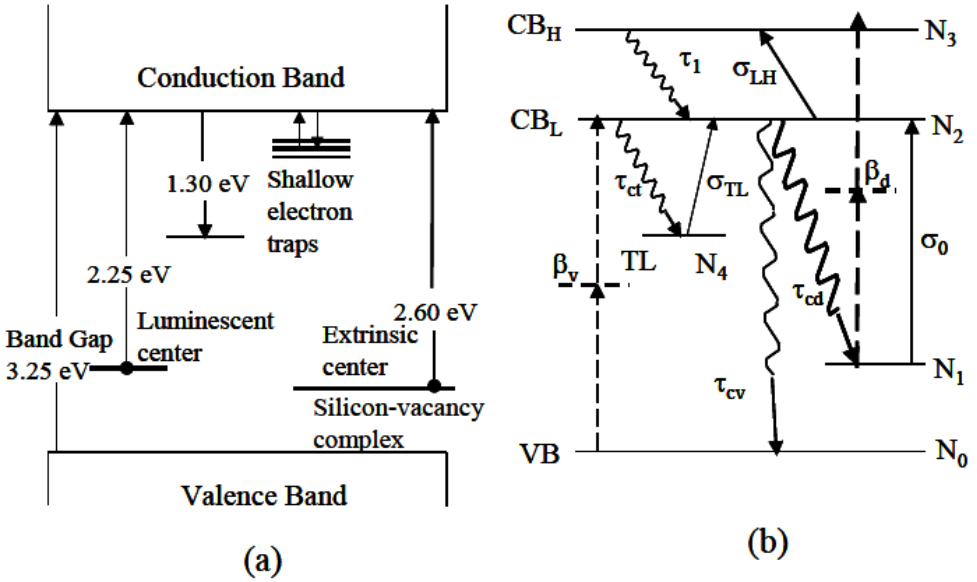

Fig 6. (a) Band model of BSO with all possible photo induced excitation and relaxation possibilities and (b) the equivalent five level diagram used for the modeling

charge carriers from the extrinsic silicon-vacancy center deep into the conduction band is generally overlooked while estimating the nonlinear absorption process. The presence of luminescence center and the shallow electron traps in BSO makes it a complex material to be modelled as a simple two-parabolic band model predicting a scaling relation for the degenerate TPA coefficient for both semiconductors and dielectric materials with gaps ranging from 1.4 to 3.7 eV [28,108,95,109]. In addition, the shallow traps are well-known to contribute to absorption. $BaTiO_3$ [110] and BSO [111] have shown the excitation of charges

from shallow traps to the conduction band [112]. The domination of photogenerated carrier absorption with nanosecond pulsed lasers has been reported earlier [28] in direct band gap semiconductors. The transfer of the conduction electrons to trap levels and the recombination with the valance band (VB) holes increases with the number density of excited electrons in the conduction band (CB).This leads to more absorption of the electrons from the trap levels to the conduction band. However, for very short pulses (ps), transitions from lower conduction band to trap levels can be neglected. Pure TPA is reported in another crystal of sillenite family $Bi_{12}GeO_{20}$ (BGO) at 532 nm using a 16 ps pulse width Nd: YAG laser [96].

The energy band structure [88,113,114] and the equivalent five level energy diagram used to explain the nonlinear absorption are shown in Fig 6 (a) and (b), respectively.

In Fig 6, VB is the valence band, *TL* is the trap level, *DL* is the donor level, CB_L represnts the lower energy levels of the conduction band and CB_H represents the higher energy levels of the conduction band. The following assumptions are made to explain the observed optical limiting and nonlinear absorption behavior of these crystals: (i) Extrinsic silicon-vacancy center is taken as donor level. Two paths of TPA are taken into consideration one from *VB* to *CB* and the other from donor level to *CB*. (ii) All the shallow and deep trap levels from which light induced absorption are considered to be originating from a single trap level (*TL*). (iii) Recombination rate of excited levels with valance-holes from the deep level of the crystal is exceptionally small [101]. (iv) Thermal excitation/decay effects are neglected in the modeling as they are of the time scale of few ms to s. The extrinsic center (silicon–vacancy complex) is considered as N_1 from where the photo absorption is possible. The shallow traps, deep traps and secondary photorefractive centers are taken as *TL* (N_4). σ_{LH} and τ_1 represent the contributions of free-carrier absorption coefficient and recombination times, respectively within the conduction band. All these processes were incorporated in the rate equations as given below:

$$\frac{dN_0}{dt} = \frac{\beta_v I^2}{2\hbar\omega} + \frac{N_2}{\tau_{CV}} \tag{1}$$

$$\frac{dN_1}{dt} = \frac{\beta_d I^2}{2\hbar\omega} - \frac{\sigma_0 I N_1}{\hbar\omega} + \frac{N_2}{\tau_{CD}} \tag{2}$$

$$\frac{dN_2}{dt} = \frac{\beta_v I^2}{2\hbar\omega} + \frac{\sigma_0 I N_1}{\hbar\omega} - N_2\left(\frac{1}{\tau_{CV}} + \frac{1}{\tau_{CD}} + \frac{1}{\tau_{CT}}\right) + \frac{N_3}{\tau_1} - \frac{\sigma_{LH} I N_2}{\hbar\omega} \pm \frac{\sigma_{TL} I N_4}{\hbar\omega} \tag{3}$$

$$\frac{dN_3}{dt} = \frac{\beta_d I^2}{2\hbar\omega} + \frac{\sigma_{LH} I N_2}{\hbar\omega} - \frac{N_3}{\tau_1} \tag{4}$$

$$\frac{dN_4}{dt} = -\frac{\sigma_{TL} I N_4}{\hbar\omega} + \frac{N_2}{\tau_{CT}} \tag{5}$$

where σ_0 is the absorption cross-section from the donor levels, β_v is the two photon absorption coefficient from the valence band to the conduction band, β_d is the two photon absorption coefficient from the donor levels to the higher conduction band leading to an effective two photon absorption coefficient, $\beta_{eff} = \beta_v + \beta_d$, σ_{TL} is the charge carrier absorption cross-section from the trap levels (TL) to the lower conduction band (CB_L), σ_{LH} is the free carrier absorption cross-section within the conduction band similar to the intraband absorption. Both these absorptions are effectively considered as σ_{1eff}. N_i's are the corresponding carrier densities in different states, τ_i's are the lifetimes of the states. $1/\tau_{CT}$ is the crossing rate to TL from lower levels of conduction band CB_L to N4, $1/\tau_{CV}$ is the crossing rate from CB_L to VB, $1/\tau_{CD}$ is the crossing rate from CB_L to DL. Intensity transmitted through the sample, as measured by the open aperture z-scan method is given by

$$\frac{dI}{dz} = -\sigma_0 I N_1 - \sigma_{LH} I N_2 - \sigma_{TL} I N_4 - \beta_{eff} I^2 \tag{6}$$

$$\text{with } I = I_{00} \times \left(\frac{w_0^2}{w^2(z)}\right) \times e^{-(t^2/\tau_p^2)} \times e^{-(2r^2/w^2(z))} \tag{7}$$

$$\text{and } w(z) = w_0\sqrt{1+\left(\frac{z}{z_0}\right)^2};\ z_0 = \frac{\pi w_0^2 n_0}{\lambda};\ \beta_{eff} = \beta_v + \beta_d$$

where I_{00} is the peak intensity, w_0 is the beam waist at focus, $w(z)$ is the spot size along the propagation direction, z_0 is the Rayleigh range of the focused beam and τ_p is the laser pulse duration. The refractive index n_0 of BSO at 532, 600 and 683 nm and is taken as 2.6, 2.55, and 2.52 respectively [116]. The differential equations are solved numerically using Runge-Kutta fourth order method. The carrier density [117] of the extrinsic absorption center N_1 is taken as ~ 10^{19} cm^{-3}. At higher intensities, BSO shows nanosecond timescale relaxation rates [118]. Nanosecond and picosecond recombination rates have been also reported for $KNbO_3$ [119,120] and $BaTiO_3$ [121] at higher intensities. Since the intensities used in the present study are high (> 10^8 Wcm^{-2}) for linear optical effects, the following relaxation (recombination) times, τ_1 = 0.1psec, τ_{CD} = 10 nsec, and τ_{CV} = 10 nsec [108,109] are used for the theoretical modeling. The excited charge carrier relaxation τ_{CT} is taken as ~ 60 psec from the pump-probe measurements.

Table 3. Nonlinear absorption cross-sections of BSO and BSO:Fe at the three excitation wavelengths of 532 nm, 600 nm and 683 nm.

λ_{ex} (nm)	β_{eff} (cm/GW)	BSO		BSO:Fe	
		Intensity ($GWcm^{-2}$)	$\sigma_{1eff}\times10^{-19}$ (cm^2)	Intensity ($GWcm^{-2}$)	$\sigma_{1eff}\times10^{-19}$ (cm^2)
532	4.47	0.21	15	0.36	41
		0.70	21	0.67	91.8
		1.23	43	---	---
600	5.02	0.54	16.8	0.43	39.2
		0.98	39.4	0.94	54
683	4.36	0.31	8.0	0.26	10.5
		0.52	11.0	0.41	16.5

The values of effective two-photon absorption cross-section obtained from the theoretical fits for the best fit parameters were compared with that from the well-established simple two-parabolic band model describing semiconductors and dielectric materials [28,108,109]. The scaling relation for the degenerate TPA coefficient is given by

$$\beta(\omega) = K_{pb}\frac{\sqrt{E_p}}{n_0^2 E_g^3} F_2\left(\frac{\hbar\omega}{E_g}\right) \tag{8}$$

where E_g is the optical bandgap and K_{pb} is the Kane momentum parameter with a value of 1940 in the units of $cm/GW(eV)^{5/2}$. The dispersion of the TPA is governed by F_2, which is a function of the ratio of the photon energy to the bandgap of optically coupled states only.

$$F_2 = \frac{(2x-1)^{3/2}}{(2x)^5} \text{ for } 2x > 1 \tag{9}$$

For the energy gaps of 3.25 eV and 2.65 eV, the value of $\beta_{eff} = \beta_v + \beta_d$, for the three excitation wavelengths of 532 nm, 600 nm and 683 nm is 1.567, 5.029 and 4.466 cm/GW, respectively. These values confirmed from the open aperture Z-scan measurements with 25 ps pulses at 532 nm [124] are used to estimate the absorption from the trap levels summarized by σ_{1eff}. From Table 3, it is evident that the overall

photo induced carrier absorption termed as trap assisted charge carrier absorption (TACCA) increases with increasing laser intensity for all the three excitation wavelengths. The iron doping has resulted in enhanced $\sigma_{1\text{eff}}$ by a factor of 1.25 to 4 confirming that the BSO crystals are a very good candidates for nonlinear absorption applications.

4 Conclusion

This review shows that the undoped and doped BSO crystals show an excellent broadband nonlinear response in the visible wavelength region. Low limiting thresholds and high damage threshold with iron doping makes these overlooked single crystalline photorefractive material suitable for limiting purposes even for short pulse duration and high energy sources over broadband region. The crystals showed a very strong nonlinear absorption with major contribution from TPA assisted by intraband carrier absorption and charge carrier absorption from trap levels. In view of the recent developments of material synthesis leading to nanocrystals, the photorefractive materials can be synthesized in nanoform that can be dispersed into different films paving the way for a large area application. Moreover, the nano crystals are potential candidates to invoke nonlinear scattering that can augment the inherent TPA and TACCA.

Acknowledgements

The research described in this publication was made possible by the persistent efforts of Prof. D. Narayana Rao, popular as DNR, and his sheer determination to explore the unexplored against any and all odds. His constant guidance during my Ph D helped me to get best thesis presentation award at National Laser Symposium-2005, which has been a turning point of my career.

References

1. Blombergen N, From nanosecond to femtosecond science, *Rev Mod Phys*, 71(1999) S283–S287.
2. Hecht J, Solid-state high-energy laser weapons, *Optics & Photonics news*, 14(2003)42–47.
3. Fatima N, Pramod A G, Ramesh P, Krishnakanth K N, Jagannath G, Rao S V, Nadaf Y F, Efficacy of Eu^{3+} on improving the near–infrared optical nonlinearities and optical limiting properties of antimony sodium borate glasses, *J Non-Cryst Solids*, 556(2021)120566; doi.org/10.1016/j.jnoncrysol.2020.120566.
4. Das B C, Reji N, Philip R, Optical limiting behavior of the natural dye extract from Indigofera Tinctoria leaves, *Opt Mater*, 114(2021)110925; doi.org/10.1016/j.optmat.2021.110925.
5. Hegde T A, Dutta A, Girisun T C S, Vinitha G, A novel chlorocadmate hybrid cocrystal delivering intermolecular charge transfer enhanced nonlinear optical properties and optical limiting, *Opt Mater*, 17(2021)111194; doi.org/10.1016/j.optmat.2021.111194.
6. Sivasubramani V, Arumugam R, Mohankumar V, Senthil P M, Ramasamy P, Synthesis, crystal growth, physico-chemical and quantum chemical investigations on 2A5NPTCA single crystal: A promising candidate for NLO and optical limiting applications, *J Mole Struct*, 1243(2021)130715; doi.org/10.1016/j.molstruc.2021.130715.
7. Reena G, Ambika D, A review on the development of optical limiters from homogeneous to reflective 1-D photonic crystal structures, *Opt Laser Technol*, 141(2021)107144; doi.org/10.1016/j.optlastec.2021.107144.
8. Jagannathan A, Rajaramakrishna R, Rajashekara K M, Jagannath G, Pattar V K, Rao S V, Eraiah B, Jagadeesha A V, Kaewkhao J, Kothan S, Investigations on nonlinear optical properties of gold nanoparticles doped fluoroborate glasses for optical limiting applications, *J Non-Cryst Solids*, 538(2020)120010; doi.org/10.1016/j.jnoncrysol.2020.120010.
9. John J, Chalana S R, Pillai V P M, Joseph J, Muthunatesan S, Ragavendran V, Tiwari G, Characterization and optical limiting behavior of BaSnO3 powder prepared by the conventional solid-state method, Materials Today: Proceedings, Vol 29, Part 4, (2020)1091-1097.
10. Abad M G G, Mahdieh M, Veisi M, Nadjari H, Mahmoudi M, Coherent control of Optical limiting in atomic systems; *Sci Rep*, 10(2020)2756; doi. org/10.1038/s41598-020-59425-1.

11. Rajeev Kumar, Ajay Kumar, Nancy Verma, Philip R, Sahoo B, FeCoCr alloy-nanoparticle embedded bamboo-type carbon nanotubes for non-linear optical limiting application, *J Alloys Compd*, 849(2020)156665; doi.org/10.1016/j.jallcom.2020.156665.
12. Sreenath M C, Hubert Joe I, Rastogi V K, Third-order optical nonlinearities of 1,5-Diaminoanthraquinone for optical limiting application, *Opt Laser Technol*, 108 (2018)218–234.
13. Zhengguo X, Yufang S, Ru S, Ge J, Li Z, Fang Y, Wu X, Yang J, Zhao M, Song Y, Ultrafast broadband optical limiting in simple pyrene-based molecules with high transmittance from visible to infrared regions, *J Mater Chem C*, 4(2016)4647–4653.
14. Haleshappa D, Jayarama A, Quah C K, Huey C K, A novel bromo-substituted thiophene based centrosymmetric crystals: Thermal, mechanical, and third order NLO properties for the optical limiting applications, *Physica B Condens Matter*, 585(2020)412083; doi.org/10.1016/j.physb.2020.412083
15. Vinaya P P, Prabhu A N, Bhat K S, Upadhyaya V, Synthesis, growth and characterization of a long-chain π-conjugation based methoxy chalcone derivative single crystal; a third order nonlinear optical material for optical limiting applications, *Opt Mater*, 89(2019)419–429.
16. Umarani P, Raja C R, Exploring the influence of charge transfer interactions on third-order optical nonlinearity, physicochemical characterization and optical limiting behaviour of (4-Methoxyphenyl) methanaminium chloride single crystal for photonic applications, *Optik*, 171(2018)326–336.
17. Sutherland R, Pachter R, Hood P, Hagan D J, Lewis K, Perry J W, (eds). Materials for Optical limiting II, Mater. Res Soc Proc (MRS, Pittsburrgh), 2001, p 479.
18. Stryland E W V, Soileau M J, Ross S, Hagan D J, Passive Optical Limiting: Where are we ?, *Nonlinear Optics*, 21(1999)29–38.
19. Hollins R C, Materials for Optical Limiters, *Curr Opin Solid State Mater Sci*, 4(1999)189–196.
20. Guo J, Chang T Y, McMichael I, Ma J, Hong J H, Light-controlled electro-optic power limiter with a $Bi_{12}SiO_{20}$ crystal, *Opt Lett*, 24(1999)981–983.
21. Frey R, Flytzanis C, Optical limitation in resonant Faraday media, *Opt Lett*, 25(2000)838–840.
22. Becker E V, Romanova E A, Melnikov L A, Benson T M, Sewell P, All-optical power limiting in waveguides with periodically distributed Kerr-like non-linearity, *Appl Phys B*, 73(2001)531–534.
23. Pelinovsky D, Sears J, Brzozowski L, Sargent E H, Stable all-optical limiting in nonlinear periodic structures I. Analysis, *J Opt Soc Am B*, 19(2002)43–53.
24. Pelinovsky D, Sargent E H, Stable all-optical limiting in nonlinear periodic structures. II. Computations, *J Opt Soc Am B*, 19(2002)1873–1889.
25. Y -P Sun, J E Riggs, Organic and inorganic optical limiting materials. From fullerenes to nanoparticles, *Int Rev Phys Chem*, 18(1999)43–90.
26. Y -P Sun, J E Riggs, K B Henbest, R B Martin, Nanomaterials as optical limiters, *J. Nonlinear Opt. Physics & Materials.*, 9(2000)481–503.
27. Tutt L W, Boggess T F, A review of optical limiting mechanisms and devices using organics, fullerenes, semiconductors and other materials, *Prog Quant Electron*, 17(1993)299–338.
28. Stryland E W V, Vanherzeele H, Woodall M A, Soileau M J, Smirl A L, Guha S, Boggess T F, Two Photon Absorption, Nonlinear Refraction, and Optical Limiting in Semiconductors, *Opt Engg*, 24(1985)613–623.
29. Joshi M P, Swiatkiewicz J, Xu F, Prasad P N, Reinhardt B A, Kannan R, Energy transfer coupling of two-photon absorption and reverse saturable absorption for enhanced optical power limiting, *Opt Lett*, 23(1998)1742–1744.
30. Hernandez F E, Yang S, Stryland E W V, Hagan D J, High-dynamic-range cascaded-focus optical limiter, *Opt Lett*, 25(2000)1180–1182.
31. Walker A C, Kar A K, Ji W, Keller U, Smith S D, All-optical power limiting of CO_2 laser pulses using cascaded optical bistable elements, *Appl Phys Lett*, 48(1986)683–685.
32. Sani E, Papi N, Mercatelli L, Barison S, Agresti F, Rossi S, Dell'Oro A, Optical limiting of carbon nanohorn-based aqueous nanofluids: A systematic study, *Nanomaterials*, 10(2020)2160; doi.org/10.3390/nano10112160.

33. Leite R C C, Porto S P S, Damen T C, The thermal lens effect as a power-limiting device, *Appl Phys Lett*, 10(1967)100–102.
34. Justus B L, Campillo A J, Huston A L, Thermal-defocusing/scattering optical limiter, *Opt Lett*, 19(1994)673–675.
35. Bunning T J, Natarajan L V, Schmitt M G, Epling B P, Crane R L, Optical limiting in solutions of diphenyl polyenes, *Appl Opt*, 30(1991)4341-4349.
36. Justus B L, Huston A L, Campillo A J, Broadband thermal optical limiter, *Appl Phys Lett.*, 63(1993)1483–1485.
37. Chari R, Mishra S R, Rawat H S, Oak S M, Reverse saturable absorption and optical limiting in indanthrone dyes, *Appl Phys B*, 62(1996)293–297.
38. Hoffman R C, Stetyick K A, Potember R S, McLean D C, Reverse saturable absorbers: indanthrone and its derivatives, *J Opt Soc Am B*, 6(1989)772–777.
39. Przhonska O V, Lim J H, Hagan D J, Stryland E W V, Bonder M V, Slominsky Y L, Nonlinear light absorption of polymethine dyes in liquid and solid media, *J Opt Soc Am B*, 15(1998)802–809.
40. Hughes S, Spruce G, Wherrett B S, Welford K R, Lloyd A D, The saturation limit to picosecond, induced absorption in dyes, *Opt Commun*, 100(1993)113–117.
41. Hughes S, Wherrett B, Multilevel rate-equation analysis to explain the recent observations of limitations to optical limiting dyes, *Phys Rev A*, 54(1995)3546; doi.org/10.1103/PhysRevA.54.3546.
42. Rao D N, Blanco E, Rao S V, Aranda F J, Rao D V G L N, Tripathy S, Akkara J A, A comparative study of C_{60}, Pthalocyanine, and Porphyrin for optical limiting over the visible region, *J Sci Ind Res*, 57(1998)664-667.
43. Hagan D J, Stryland E W V, Wu Y Y, Wei T H, Sheik-Bahae M, Said A A, Mansour K, Young J, Soileau M J, Materials for Optical Switches, Isolators, and Limiters, *Proc of SPIE*, 1105(1989)103–113.
44. Philip R, Kumar G R, Sandhyarani N, Pradeep T, Picosecond optical nonlinearity in monolayer-protected gold, silver, and gold-silver alloy nanoclusters, *Phys Rev B*, 62(2000)13160; doi.org/10.1103/PhysRevB.62.13160.
45. Stryland E W V, Wu Y Y, Hagan D J, Soileau M J, Mansour K, Optical limiting with semiconductors, *J Opt Soc Am B*, 5(1988)1980–1988.
46. Hagan D J, Stryland E W V, Soileau M J, Wu Y Y, Guha S, Self-protecting semiconductor optical limiters, *Opt Lett*, 13(1988)315–317.
47. Vijaya R, Murti Y V G S, Vijayaraj T A, Sundararajan G, Optical limiting action in poly(*para*-methoxy phenylacetylene), *Curr Sci*, 72(1997)507–508.
48. Staromlynska J, McKay T J, Bolger J A, Davy J R, Evidence for broadband optical limiting in a Pt:ethynyl compound, *J Opt Soc Am B*, 15(1998)1731–1736.
49. Allan G R, Labergerie D R, Rychnovsky S J, Boggess T F, Smirl A F, Tutt L W, Picosecond reverse saturable absorption in King's complex *J Phys Chem*, 96(1992)6313–6317.
50. Brzozowski L, Sargent E H, Nonlinear Disordered Media for Broad-Band Optical Limiting, *IEEE J Quantum. Electron*, 36(2000)1237–1242.
51. Fang G, Song Y, Wang Y, Zhang X, Li, Song L-C, Liu P-C, Z-scan of excited-state nonlinear materials with reverse saturable absorption, *Opt Commun*, 183(2000)523–527.
52. Zhou J, Pun E Y B, Zhang X H, Nonlinear optical refractive indices and absorption coefficients of α,β-unsaturated ketone derivatives, *J Opt Soc Am B*, 18(2001)1456–1463.
53. Morel Y, Zaccaro J, Ibanez A, Baldeck P L, Nonlinear absorption and optical limiting properties of the 2-amino-5-nitropyridinium dihydrogenophosphate hybrid crystal, *Opt Commun*, 201(2002)457–464.
54. Sun Z, Tong M, Zeng H, Ding L, Wang Z, Dai J, Bian G, Xu Z, Nanosecond reverse saturable absorption and optical limiting in $(Me_4N)_2[Cd(dmit)(Sph)_2]$, *J Opt Soc Am B*, 18(2001)1464–1468.
55. Boggess T F, Moss S C, Boyd I W, Smirl A L, Nonlinear-optical energy regulation by nonlinear refraction and absorption in silicon, *Opt Lett*, 9(1984)291–293.
56. Boggess T F, Smirl A L,Moss S C, Boyd I W, Stryland E W V, Optical limiting in GaAs, *IEEE J Quantum Electron*, 21(1985)488–494.
57. Ji W, Kukaswadia A K, Feng Z C, Tang S H, Self-defocusing of nanosecond laser pulses in ZnTe, *J Appl Phys*, 75(1994)3340–3343.

58. Kiran P P, Reddy D R, Maiya B G, Rao D N, Third order nonlinearity and optical limiting studies in phosphorus (V) porphyrins with charge transfer states, *Opt Mater*, 21(2002)565–568.
59. Kiran P P, Srinivas N K M N, Reddy D R, Maiya B G, Sandhu A S, Dharmadhikari A K, Kumar G R, Rao D N, Heavy atom effect on nonlinear absorption and optical limiting characteristics of 5,10,15,20-(tetratolyl) porphyrinato phosphorus (V) dichloride, *Opt Commun*, 202(2002)347–352.
60. Kiran P P, Reddy D R, Maiya B G, Dharmadhikari A K, Kumar G R, Rao D N, Enhanced optical limiting and nonlinear absorption properties of azoarene appended phosphorus (V) tetratolylporphyrins, *Appl Opt*, 41(2002)7631–7636.
61. Rao S V, Kiran P P, Giribabu L, Ferrari M, Kurumurthy G, Krishna B M, Sekhar H, Rao D N, Anomalous nonlinear absorption behavior in an unsymmetrical phthalocyanine studied near 800 nm using femtosecond and picosecond pulses, *Nonlinear Opt Quantum Opt*, 40(2010)223–234.
62. Kiran P P, Reddy D R, Maiya B G, Dharmadhikari A K, Kumar G R, Rao D N, Contribution of two-photon and excited state absorption in 'axial-bonding' type hybrid porphyrin arrays under resonant electronic excitation, *Chem Phys Lett*, 418(2006)442– 447.
63. Kiran P P, Reddy D R, Maiya B G, Dharmadhikari A K, Kumar G R, Rao D N, Nonlinear absorption properties of 'axial-bonding' type hybrid porphyrin arrays based on Sn(IV)TTP scaffold, *Opt Commun*, 252(2005)150–161.
64. Kiran P P, Bhakta B N S, Rao D N, De G, Nonlinear optical properties and surface plasmon enhanced optical limiting properties of Ag-Cu nanoclusters co-doped in SiO_2 sol-gel films, *J Appl Phys*, 96(2004)6717-6723.
65. Kiran P P, De G, Rao D N, Nonlinear optical properties of copper and silver nanoclusters in SiO_2 Sol-Gel films, *IEE Proc.-Circuits Devices Syst*, 150(2003)559–562.
66. Lad A D, Kiran P P, Kumar G R, Mahamuni S, Three-photon absorption in ZnSe and ZnSe/ZnS quantum dots, *Appl Phys Lett*, 90(2007)133113; doi.org/10.1063/1.2714994.
67. Lad A D, Kiran P P, More D, Kumar G R, Mahamuni S, Two-photon absorption in ZnSe and ZnSe/ZnS core/shell quantum structures, *Appl Phys Lett*, 92(2008)043126; doi.org/10.1063/1.2839400.
68. Nag A, Kumar A, Kiran P P, Chakraborty S, Kumar G R, Sarma D D, Optically Bi-functional Hetero-Structured Nanocrystals, *J Phys Chem C*, 112(2008)8229–8233.
69. Kiran P P, Rao S V, Ferrari M, Krishna B M, Sekhar H, Alee S, Rao D N, Enhanced optical limiting performance through nonlinear scattering in nanoparticles of CdS, co-doped Ag-Cu, and BSO, *Nonlinear Opt Quantum Opt*, 40(2010)183–191.
70. Sekhar H, Kiran P P, Rao D N, Structural, linear and enhanced nonlinear optical properties of $Bi_{12}SiO_{20}$ Nanocrystals, *Mater Chem Phys*, 130(2011)113–120.
71. Sekhar H, Kiran P P, Rao D N, Nonlinear optical properties of BSO nanoparticles dispersed in PMMA matrix, *Proc SPIE* 7712, (2010); doi.org/10.1117/12.854204.
72. Yeh P, Introduction to photorefractive nonlinear optics, (John-Wiley, New York), 1993.
73. Yu F T S, Yin S, (eds), Photorefractive Optics. (Academic Press), 2000.
74. Gunter P, Holography, coherent light amplification and optical phase conjugation with photorefractive materials, *Phys Rep*, 93(1982)199–299.
75. Golomb M C, Whole beam method for photorefractive nonlinear optics, *Opt Commun*, 89(1992)276–282.
76. Huignard J P, Survey of photorefractive nonlinear crystals and their applications, *Proc SPIE*, 1127(1989)205; doi. doi.org/10.1117/12.961421.
77. Shaw K D, Golomb M C, Optical bistability in photorefractive four-wave mixing, *Opt Commun*, 65(1988)301–305.
78. Hermann J A, Staromlynska J, Trends in optical switches, limiters and discriminators, *Int J Nonlinear Opt Phys*, 2(1993)271–337.
79. Huot N, Jonathan J, Roosen G, Validity of the three-charge-state model in photorefractive $BaTiO_3$:Rh at 1.06 μm in the cw regime, *Appl Phys B*, 65(1997)489–493.
80. Krose H, Scharfschwerdt R, Schirmer O F, Hesse H, Light-induced charge transport in $BaTiO_3$ via three charge states of rhodium, *Appl Phys B*, 61(1995)1–7.
81. Buse K, Light-induced charge transport processes in photorefractive crystals II: Materials, *Appl Phys B*, 64(1997)391–407.

82. Mazur A, Stevendaal U V, Buse K, Weber M, Schirmer O F, Hesse H, Kratzig E, Light-induced charge transport processes in photorefractive barium titanate crystals doped with iron, *Appl Phys B*, 65(1997)481–487.
83. D N Rao, P P Kiran, Optical limiting studies of BSO crystal using a nanosecond laser source, *Nonlinear Optics*, 27(2001)347–355.
84. (a) Linde D, Glass A M, Rodgers K F, Multiphoton photorefractive processes for optical storage in $LiNbO_3$, *Appl Phys Lett*, 25(1974)155; doi.org/10.1063/1.1655420.

    (b) Linde D, Glass A M, Rodgers K F, High−sensitivity optical recording in KTN by two−photon absorption, *Appl Phys Lett*, 26(1975)22; doi.org/10.1063/1.87974.
85. Chen C T, Kim D M, Linde D V, Efficient pulsed photorefractive process in $LiNbO_3$:Fe for optical storage and deflection, *IEEE J Quantum Electron*, 16(1980)126-129.
86. Aithal P S, Kiran P P, Rao D N, Optical Limiting Studies in Photorefractive Pure and Iron-Doped $Bi_{12}SiO_{20}$ Crystals, *J Nonlinear Opt Phys Mater*, 9(2000)217-225..
87. Egorysheva A V, Burkov V I, Kargin Y F, Vasilev A Y, Volkov V V, Skorikov V M, Spectroscopic properties of $Bi_{12}SiO_{20}$ and $Bi_{12}TiO_{20}$ crystals doped with Mn, Mn + P, Cr +P, Cr + Ga, and Cr + Cu, *Inorg Mater*, 37(2001)817–824.
88. Attard A E, Photoconductive and photorefractive effects in BSO, *Appl Opt*, 28(1989)5169–5174.
89. Benjelloun N, Tapiero M, Zielenger J P, Launay J C, Marsaud F, Characterization of deep levels in $Bi_{12}GeO_{20}$ by photoinduced current transient spectroscopy, *J Appl Phys*, 64(1988)4013–4023.
90. Grabmaier B C, Oberschmid R, Properties of Pure and Doped $Bi_{12}GeO_{20}$ and $Bi_{12}SiO_{20}$ Crystals, *Phys Stat Sol (a)*, 96(1986)199–210.
91. Attard A E, Fermi level shift in $Bi_{12}SiO_{20}$ via photon-induced trap level occupation, *J Appl Phys*, 71(1992)933–937.
92. A Mazur, C Veber, O F Schirmer, C Kuper, H Hesse, Light-induced charge transport processes in photorefractive $Ba_{0.77}Ca_{0.23}TiO_3$ doped with iron, *J Appl Phys*, 85(1999)6751–6757.
93. Gospodinov M, Doshkova D, Growth and optical properties of iron, cobalt and nickel doped bismuth silicate crystals, *Mater Res Bull*, 29(1994)681–686.
94. Nagao Y, Mimura Y, Properties of $Bi_{12}SiO_{20}$ single crystals containing first row transition metal, *Mat Res Bull*, 24(1989)239–246.
95. Nesheva D, Aneva Z, Gospodinov M, Traps and recombination centers in pure and Co-doped $Bi_{12}SiO_{20}$ crystals, *J Phys Chem Solids*, 54(1993)857–862.
96. Taheri B, Holmstorm S A, Powell R C, Song J J, Munoz F, Foldvari I, A Peter, Nonlinear absorption of laser light in $Bi_{12}GeO_{20}$ single crystals, *Opt Mater*, 3 (1994)251–255.
97. Aggarwal M D, Wang W S, Choi J, Cochrane J C, Wang Z Y, Morphology and formation of the color core of $Bi_{12}SiO_{20}$ crystals grown by the Czochralski method, *J Cryst Growth*, 137(1994)132–135.
98. Mokrushina E V, Bryushinin M A, Kulikov V V, Petrov A A, Sokolov I A, Photoconductive properties of photorefractive sillenites grown in an oxygen-free atmosphere, *J Opt Soc Am B*, 16(1999)57–62.
99. Mazur A, Schirmer O F, Mendricks S, Optical absorption and light-induced charge transport of Fe^{2+} in $BaTiO_3$, *Appl Phys Lett*, 70(1997)2395–2397.
100. Kovacs L, Sommerfeldt R, Ming Y, Kratzig E, Light-induced charge transport in $LiNbO_3$:Mg,Cr crystals, *Phys Stat Solv(a)*, 113(1989)K75–K78.
101. Liu A, Lee M, Hesselink L, Lee S -H, Lim K -S, Light-induced absorption of cerium-doped lead barium niobate crystals, *Opt Lett*, 23(1998)1618–1620.
102. Nesheva D, Aneva Z, Levi Z, Some properties of $Bi_{12}SiO_{20}$:Fe doped crystals, *J Phys Chem Solids*, 55(1994)889–894.
103. Kumar V N, Spectral interferometry a study of the degree of coherence in the space frequency domain and the applications, Ph D Thesis, University of Hyderabad, India, January 1997.
104. Rao S V, Studies of excited state dynamics, third order optical nonlinearity and nonlinear absorption in C60, porphyrins and phthalocyanines using incoherent laser spectroscopy, Ph D Thesis, University of Hyderabad, India, January 2001.

105. James D B, McEwan K J, Bubble and refractive processes in carbon suspensions, *Nonlinear Opt*, 21(1999)377–389.
106. Kay T J M, Staromlynska J, Davy J R, Bogler J, Cross sections for excited-state absorption in a Pt:ethynyl complex, *J Opt Soc Am B*, 18(2001)358–362.
107. Sheik-Bahae M, Said A A, Wei T H, Hagan D J, Stryland E W V, Sensitive measurement of optical nonlinearities using a single beam, *IEEE J Quant Electron*, 26(1990)760–769.
108. Stryland E W V, Woodall M A, Vanerzeele H, Soileau M J, Energy band-gap dependence of two-photon absorption, *Opt Lett*, 10(1985)490–492.
109. Sheik-Bahae M, Hagan D J, Stryland E W V, Dispersion and band-gap scaling of the electronic Kerr effect in solids associated with two-photon absorption, *Phys Rev Lett*, 65(1990)96–100.
110. Brost G A, Motes R A, Rotge J R, Intensity-dependent absorption and photorefractive effects in barium titanate, *J Opt Soc Am B*, 5(1988)1879–1885.
111. Zheludev N I, Ruddock I S, Illingworth R, Intensity dependence of thermal nonlinear optical activity in crystals. *Appl Phys B*, 49(1989)65–67.
112. Tayebati P, Mahgerefteh D, Theory of the photorefractive effect for $Bi_{12}SiO_{20}$ and $BaTiO_3$ with shallow traps, *J Opt Soc Am B*, 8(1991)1053–1064.
113. Peltier M, Micheron, Volume hologram recording and charge transfer process in $Bi_{12}SiO_{20}$ and $Bi_{12}GeO_{20}$, *J Appl Phys*, 48(1977)3683–3690.
114. Hou S L, Lauer R B, Aldrich R E, Transport processes of photoinduced carriers in $Bi_{12}SiO_{20}$, *J Appl Phys*, 44(1973)2652–2658.
115. Stevendaal U V, Buse K, Malz H, Kratzig E, Persistent light-induced absorption in oxidized iron-doped barium titanate crystals, *Opt Lett*, 24(1999)908–910.
116. R E Aldrich, S L Hou, M L Harvill, Electrical and Optical Properties of $Bi_{12}SiO_{20}$, *J Appl Phys*, 42(1971)493-494.
117. Sylla M, Rouede D, Chevalier R, Phu X N, Rivoire G, Picosecond nonlinear absorption and phase conjugation in BSO and BGO crystals, *Opt Commun*, 90(1992)391–398.
118. Zgonik M, Biaggio I, Bertele U, Gunter P, Degenerate four-wave mixing in $KNbO_3$: picosecond and photorefractive nanosecond response, *Opt Lett*, 16(1991)977–979.
119. Biaggio I, Zgonik M, Gunter P, Photorefractive effects induced by picosecond light pulses in reduced $KNbO_3$, *J Opt Soc Am B*, 9(1992)1480–1487.
120. Ye P, Blouin A, Demers C, Roberge MM D, Wu X, Picosecond photoinduced absorption in photorefractive $BaTiO_3$, *Opt Lett*, 16(1991)980–982.
121. Boggess T F, White J O, Valley G C, Two-photon absorption and anisotropic transient energy transfer in $BaTiO_3$ with 1-psec excitation, *J Opt Soc Am B*, 7(1990)2255–2258.
122. Miller A, Miller D A B, Smith S D, Dynamic non-linear optical processes in semiconductors, *Adv Phys*, 30(1981)697-800.
123. Beattie A R, Landsberg P T, Auger effect in semiconductors, *Proc Roy Soc A*, 249(1959)16; doi.org/10.1098/rspa.1959.0003.
124. Kiran P P, Kumar G R, Rao D N, Ultrafast carrier relaxation and nonlinear absorption in $Bi_{12}SiO_{20}$ single crystal, Proc PHOTONICS-2008: International Conference on Fiber Optics and Photonics, December 13-17, 2008, IIT Delhi, India.

[*Received*: 01.06.21; *revised recd*: 16.06.2021; *accepted*: 29.06.2021]